

# Analysis of stress distribution in a thin rectangular plate by the method of caustics

J. WANG, R. C. BATRA (BLACKSBURG) and K. ISOGIMI (TSU)

WE DISCUSS some characteristics of caustics in a rectangular plate loaded by distributed in-plane loads on a part of two opposite edges with the other two edges kept traction-free. It is assumed that plane state of stress prevails in the plate. The theoretical developments are valid for an arbitrary location of the reflective plane within the plate. A good agreement is found between the computed and observed caustics. A simple inverse problem of determining the intensity of the distributed load from the size of caustics is also investigated.

## 1. Introduction

THE METHOD of caustics was first proposed by MANOGG [1] and has been employed by THEOCARIS [2, 3] and KALTHOFF [4] to ascertain stresses at singular points. The method is widely used in fracture mechanics to determine stress intensity factors under Modes I, II and III loading [5]. Here we apply this method to another kind of singular problem, namely, distributed load acting on a part of the width of a plate; this is a simplified model of loads acting on a cutting tool. The deformations and stresses will be singular at points where the distributed load jumps from zero to a finite value or vice-versa. Here we consider a thin plate subjected to in-plane distributed loads at two opposite edges with the other two edges traction-free and assume that a plane stress state prevails in the plate. We use the method of caustics to transform the stress singularity to an optical singularity and determine the stress distribution at singular points. It is assumed that the intensity of the distributed load is such that the linear elasticity theory can be used to describe deformations of the plate. The work is motivated by the desire to ascertain stresses induced in a cutting tool; however no machining problem is studied herein.

## 2. Analytical developments of caustics

Referring to Fig. 1, consider parallel rays impinging upon the plane surface of a transparent, homogeneous, and both mechanically and optically isotropic rectangular plate subjected to in-plane distributed loads on two opposite edges. The direction of the light reflected from a point on the incident surface will depend upon its deformations. This light when projected on a screen, will form caustics whose patterns will depend upon the state of stress at points on the incident surface. If the location of the plane from which the incident light is

reflected can be varied, then the state of stress at points within the body can also be ascertained by the method of caustics.

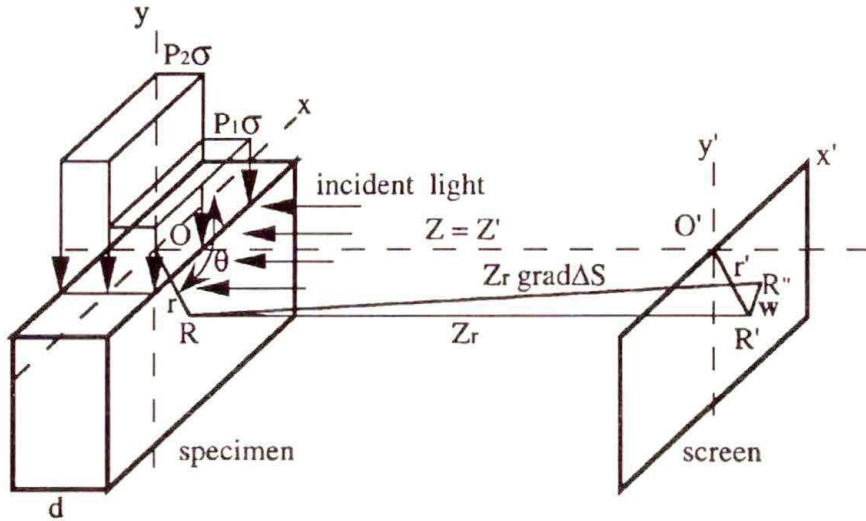


FIG. 1. A schematic sketch of the problem studied.

2.1. Optical path difference

We assume that the distributed load on the edge of a plate can be approximated by a series of step loads as shown in Fig.2. Herein we assume the distributed load to be such that points on the central plane of the plate do not move laterally. Also with the plate divided into several layers with thickness of each layer equaling the thickness of the edge over which the load intensity is constant, we presume that a plane state of stress exists within each layer. Let the plate be divided into  $n$  layers of thicknesses  $d_1, d_2, \dots, d_N$  and in-plane loads acting on their edges equal  $P_1\sigma, P_2\sigma, \dots, P_N\sigma$ , respectively. Under the action of these loads, the thickness  $d_i$  and refractive index  $n_i$  of the  $i$ -th layer ( $1 \leq i \leq N$ ) will change by  $\Delta d_i$  and  $\Delta n_i$ , respectively. We designate by subscripts  $c$  and  $m$  the central surface of the plate and the plane from which light is reflected.

A lateral displacement of a material point in the direction of increasing optical path is taken as positive. Thus under a compressive edge load, the lateral displacement of the front surface of the plate is  $-\Delta d_f$  and that of the rear surface equals  $+\Delta d_r$ . Of course, as assumed above, the lateral displacement of the central surface is zero.

As shown in Fig.2, we consider a reflective plane located at a distance of  $kd$  ( $0 \leq k \leq 1$ ) from the front surface of the plate. Measuring distances from the deformed position of the front surface, the optical path  $S_1$  to the reflective plane in the unstressed reference configuration is given by

$$(2.1) \quad S_1 = 2(\Delta d_f + nkd),$$

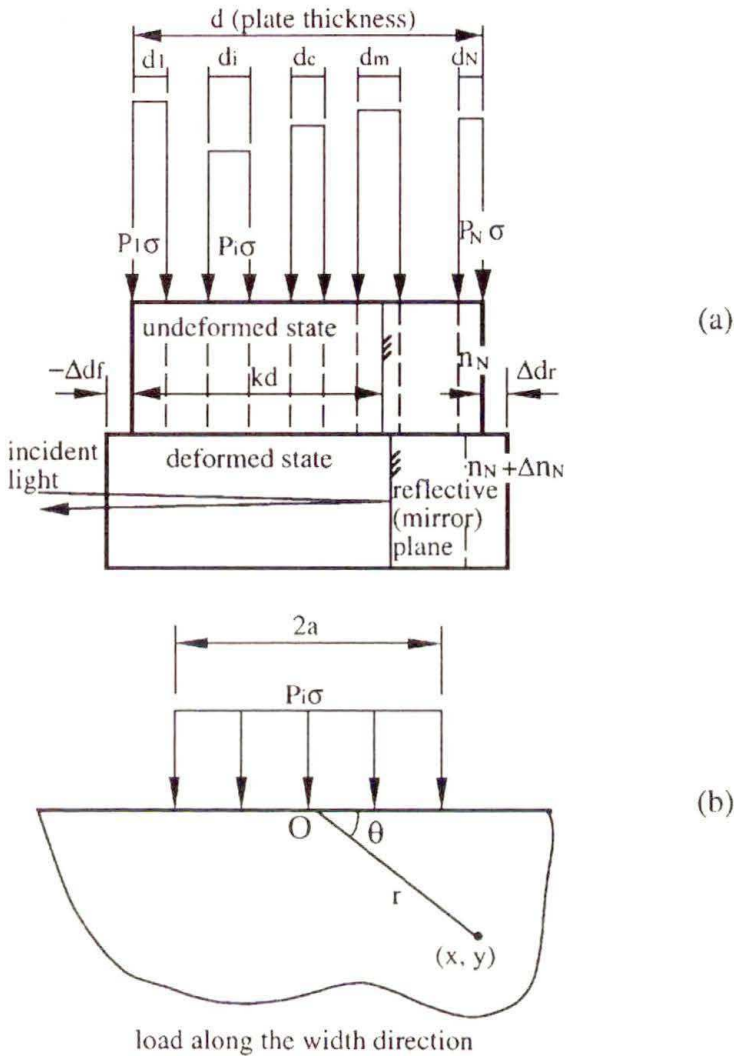


FIG. 2. a) Load distribution along the thickness of the plate; b) load distribution along the width of the plate.

where  $n$  is the refractive index of the plate material in the unstressed state and the refractive index of air equals 1. After the load is applied, the optical path will change to  $S_2$  given by

$$(2.2) \quad S_2 = 2 \left[ \sum_{i=1}^{m-1} (n + \Delta n_i)(d_i + \Delta d_i) + (n + \Delta n_m) \frac{1}{d_m} \left( kd - \sum_{i=1}^{m-1} d_i \right) (d_m + \Delta d_m) \right].$$

In writing equation (2.2) we have assumed that the reflective plane (or mirror) is located in the  $m$ -th layer. Subtracting (2.1) from (2.2) and neglecting terms of second order in  $\Delta d$  and/or  $\Delta n$ , we obtain the following formula for the optical path difference

$$(2.3) \quad \Delta S = 2 \left[ \sum_{i=1}^{m-1} (\Delta n_i d_i + n \Delta d_i) + \left( \Delta n_m + \frac{n}{d_m} \Delta d_m \right) \left( kd - \sum_{i=1}^{m-1} d_i \right) - \Delta d_f \right].$$

The variation in the thickness of the  $i$ -th layer subjected to in-plane edge loads  $P_i \sigma$  can be expressed as

$$(2.4) \quad \Delta d_i = -\frac{\nu}{E} P_i d_i (\sigma_1 + \sigma_2),$$

where  $E$  and  $\nu$  equal, respectively, Young’s modulus and Poisson’s ratio for the material of the plate, and  $\sigma_1$  and  $\sigma_2$  are the principal stresses induced at a point in the plate layer subjected to in-plane surface traction  $\sigma$  (recall that the third principal stress is zero because of the assumption of plane stress). Since the central plane is assumed not to move laterally, therefore, the displacement  $\Delta d_f$  of the front surface is given by

$$(2.5) \quad \Delta d_f = -\frac{\nu}{E} \left[ \sum_{i=1}^c P_i d_i - P_c \left( \sum_{i=1}^c d_i - \frac{d}{2} \right) \right] (\sigma_1 + \sigma_2),$$

where it has been assumed that the central plane lies in the  $c$ -th layer. For an optically isotropic  $i$ -th layer, the change in the refractive index at a point is given by

$$(2.6) \quad \Delta n_i = A P_i (\sigma_1 + \sigma_2),$$

where  $A$  is the optical constant for the plate material. Substitution from (2.4), (2.5) and (2.6) into (2.3) results in the following expression for  $\Delta S$ :

$$(2.7) \quad \Delta S = K (\sigma_1 + \sigma_2),$$

where

$$(2.8) \quad K = 2 \left\{ \left( A - n \frac{\nu}{E} \right) \sum_{i=1}^{m-1} P_i d_i + \left( kd - \sum_{i=1}^m d_i \right) \left( A P_m - n P_m \frac{\nu}{E} \right) + \frac{\nu}{E} \left[ \sum_{i=1}^c P_i d_i - P_c \left( \sum_{i=1}^c d_i - \frac{d}{2} \right) \right] \right\}.$$

## 2.2. Equation of caustics

Referring to Fig. 1, let  $R'$  be the image of  $R$  on a plane screen located at a distance  $Z_r$  from  $R$  when there is no load applied to the plate, and  $R''$  be the image of  $R$  when the plate has been deformed by in-plane loads applied at the two opposite edges. The vector  $\mathbf{w} = \overrightarrow{R'R''}$  is given by [6]

$$(2.9) \quad \mathbf{w} = Z_r \text{grad } \Delta S = K Z_r \text{grad } (\sigma_1 + \sigma_2)$$

where we have used (2.7).

Let the stress state at an arbitrary point in the plate with two opposite edges subjected to uniform in-plane tractions  $\sigma$  be described by the complex-valued function  $\phi(z)$  of the complex variable  $z = x + iy$ . Then

$$(2.10) \quad 4 \text{Re}(\phi(z)) = \sigma_1 + \sigma_2,$$

where  $\text{Re}(\phi(z))$  denotes the real part of  $\phi$ . In the complex variable notation, Eq. (2.9) becomes

$$(2.11) \quad w = 4K Z_r \bar{\phi}'(z),$$

where  $\bar{\phi}$  denotes the complex conjugate of  $\phi$ . Assuming that the origin  $O$  of the rectangular Cartesian coordinate system is located on the top surface of the undeformed plate and the applied tractions are distributed symmetrically about it,  $O'$  is its image on the screen and  $\mathbf{r} = \overrightarrow{OR}$ , then

$$(2.12) \quad \mathbf{W} = \overrightarrow{O'R''} = \mathbf{w} + \mathbf{r}.$$

However, when the incident light is not a parallel beam but a convergent beam, then Eq. (2.12) is modified to

$$(2.13) \quad \mathbf{W} = \mathbf{w} + \lambda \mathbf{r},$$

where

$$(2.14) \quad \lambda = (Z_i - Z_r)/Z_i,$$

and  $Z_i$  is the distance of the focal point of the light from the reflective plane (cf. Fig. 3). Of course, for a parallel incident beam,  $\lambda = 1$ .

In the complex plane, Eqs. (2.11) and (2.13) yield

$$(2.15) \quad W = x' + iy' = \lambda(x + iy) + 4K Z_r \bar{\phi}'(z)$$

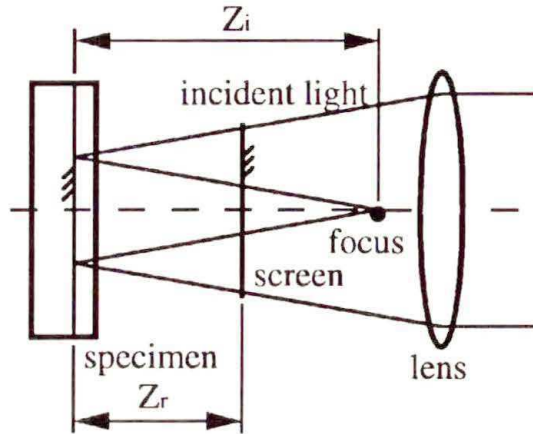


FIG. 3. A schematic sketch of the convergent light beam and illustrations of distances  $Z_i$  and  $Z_r$ .

and the condition

$$(2.16) \quad J = \frac{\partial(x', y')}{\partial(x, y)} = 0$$

for the existence of a singular point becomes

$$(2.17) \quad \left| \frac{4}{\lambda} K Z_r \phi''(z) \right| = 1.$$

Thus the caustic curve is obtained from Eqs. (2.17) and (2.15).

For the load distribution depicted in Fig. 2, Eq. (2.17) gives

$$(2.18) \quad AB = 4arC/\lambda,$$

where

$$(2.19) \quad \begin{aligned} A &= r^2 + a^2 - 2ar \cos \theta, \\ B &= r^2 + a^2 + 2ar \cos \theta, \\ C &= 2\sigma K Z_r / \pi, \end{aligned}$$

$(r, \theta)$  are the cylindrical polar coordinates of the point  $(x, y)$  (e.g. see Fig. 2), and  $2a$  is the width of the loaded region. Equation (2.15) describing a caustic curve can be written as

$$(2.20) \quad \begin{aligned} x' &= \lambda r \left( \cos \theta - \frac{1}{2} \sin 2\theta \right), \\ y' &= \lambda r \left( \sin \theta - \frac{1}{2} \cos 2\theta - \frac{1}{2} \frac{a^2}{r^2} \right). \end{aligned}$$

We identify the size of a caustic curve with the maximum horizontal distance,  $D = L_{\max}$ , between any two points on the curve. For the load applied symmetrically about  $O$ , it is reasonable to assume that the caustic curve is symmetrical about  $O'$ . Thus if points  $(r_0, \theta_0)$  and  $(r_0, -\theta_0)$  on the caustic curve determine  $D$ , then

$$(2.21) \quad D = L_{\max} = br_0,$$

where

$$(2.22) \quad b = 2\lambda \left( \cos \theta_0 - \frac{1}{2} \sin 2\theta_0 \right).$$

Equations (2.18) and (2.21) give the following relation between the applied uniform traction  $\sigma$  and the size of a caustic.

$$(2.23) \quad \sigma = \frac{\pi\lambda}{8KZ_r a} \frac{D}{b} \left[ \left( \frac{D}{b} + \frac{b}{D} a^2 \right)^2 - 4a^2 \cos^2 \theta_0 \right].$$

Knowing  $D$ , nonlinear equations (2.18) and (2.21) can be solved iteratively for  $r_0$  and  $\theta_0$ , and then  $\sigma$  can be evaluated from Eq. (2.23). Subsequently, the stress distribution at any point in the plate can be ascertained.

### 3. Experimental method

A schematic sketch of the experimental set-up is shown in Fig. 4. All of the components depicted in the figure, except for the video monitor and recording equipment, are mounted on a vibration-isolated table. A laser light from the

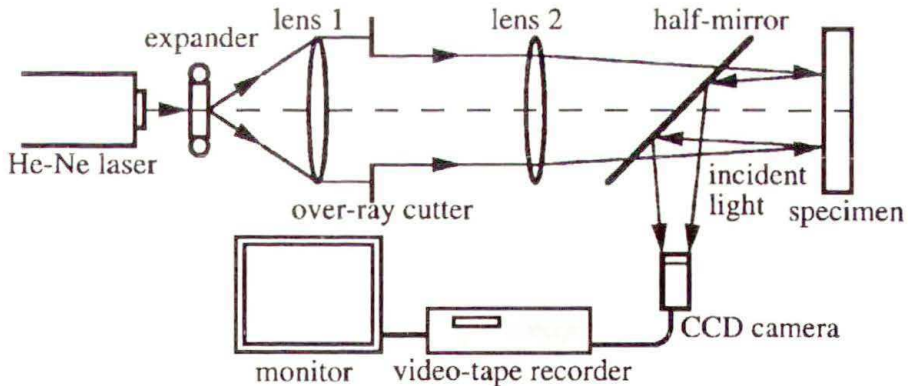


FIG. 4. A layout of the experimental apparatus.

source is expanded by the expander, changed into collimated light by lens 1 and into a convergent beam by lens 2. The region of interest with singular stress distribution in the object is illuminated with the laser light through a half-mirror.

Light falling from the object and the half-mirror is received by a CCD camera, recorded on a video-tape and monitored. The dimension ratio  $\lambda$ , defined by Eq. (2.14), of the convergent light is determined and adjusted by altering the positions of lens 2, the half-mirror and the CCD camera.

The specimen length, width and thickness equal, respectively, 63 mm, 45 mm and 6 mm and it is made of transparent acrylate. The reflective surface of the specimen is formed by vapor depositing a layer of aluminum film on either the front or the rear surface of the plate.

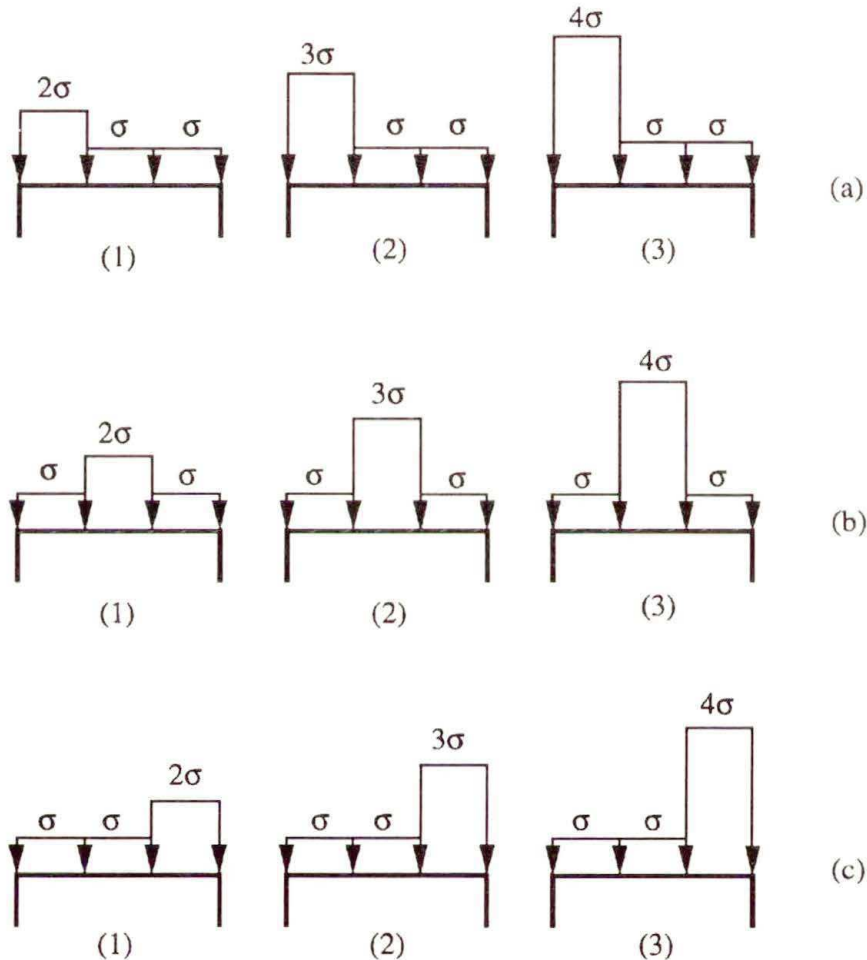


FIG. 5. Different load distributions considered.

Nine different loads described below and shown in Fig. 5 were examined. The plate thickness is divided into three equal parts; on each part the tractions are uniformly distributed and span over the middle 4.5 mm width of the plate.

#### 4. Comparison of experimental and computed results

Figure 6 shows the experimental and computed caustic curves for the three load distributions of group (a) of Fig. 5; the top, middle and bottom figures correspond respectively to load distributions 1, 2 and 3. Unless otherwise noted, the reflective plane is located on the front surface of the plate. The computed results are obtained by assigning following values to the material parameters:  $A = -0.55 \times 10^{-18} \text{ m}^2/\text{N}$ ,  $n = 1.491$ ,  $E = 1.6 \text{ GPa}$ ,  $\nu = 0.399$ . The experimentally obtained caustic curves are not completely symmetric about the center-line probably because of the slight asymmetry in the externally applied tractions. However, the experimental and computed curves look similar implying that the assumptions made in deriving the equation for a caustic curve are reasonable. In Fig. 7 we have plotted the computed and experimental values of the size of the

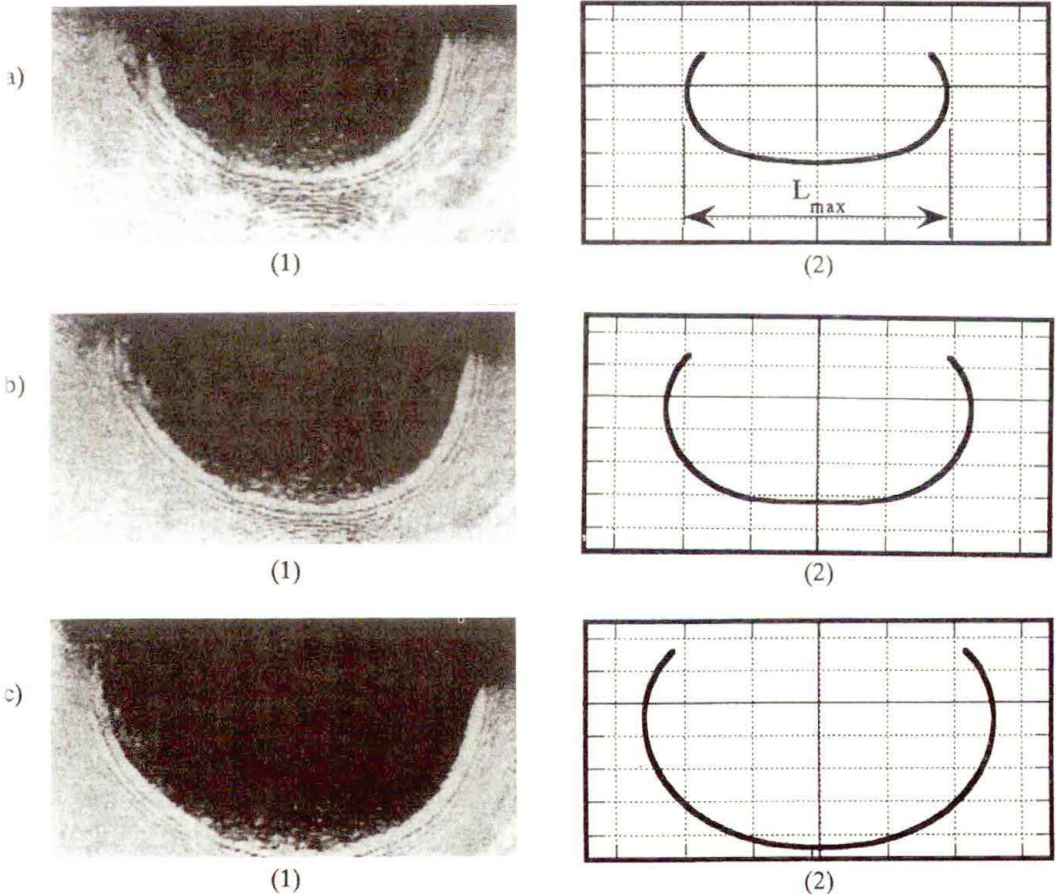


FIG. 6. Experimental (1) and computed (2) caustic curves for the three load distributions of group (a) of Fig. 5 with the reflective plane located on the front surface of the plate.

caustic curves for the load distribution of group (a) versus the maximum traction; it is clear that the two sets of values agree well with each other. The plot of the optical path difference computed from Eq. (2.7) shows that there is an affine relationship between it and the maximum traction.

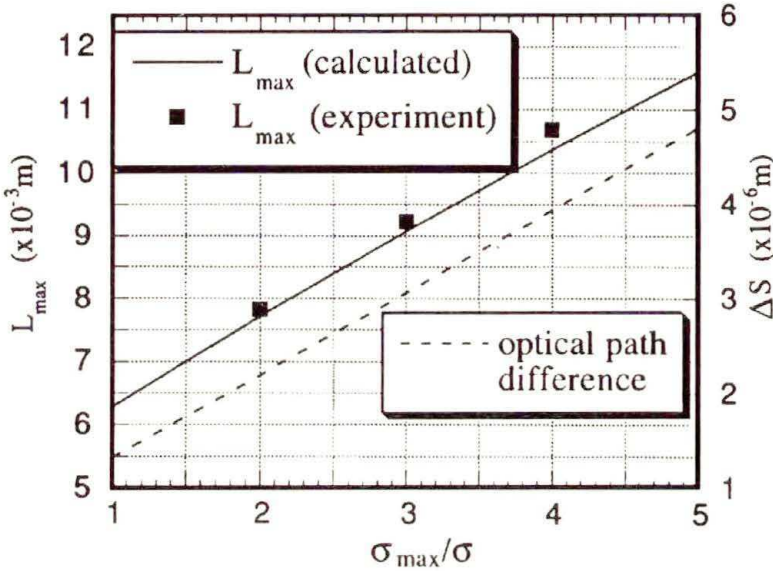


FIG. 7. Dependence of the size of the caustic curve and the computed optical path difference upon the magnitude of the maximum load.

The effect of the location of the maximum traction on the experimental and computed caustic curves is illustrated in Fig. 8 where the two sets of caustics obtained by applying the maximum traction ( $= 4\sigma$ ) on the front layer, middle layer and the rear layer (i.e. loading 3 of groups (a), (b) and (c)) are exhibited. It is clear that the shape of the caustic produced depends strongly upon the location of the maximum traction. The computed and experimental values of the size of the caustic curve versus the location of the position of  $\sigma_{\max}$  are compared in Fig. 9; the two sets of values match well with each other. Also shown in Fig. 9 is the dependence of the computed  $L_{\max}$  upon the location of  $\sigma_{\max}$  with the reflective plane located on the rear surface of the specimen. One can conclude from these results that the location of  $\sigma_{\max}$  influences strongly the size of the caustic curve only when this location is near the reflective plane. Figure 10 depicts the experimental and computed caustic curves under the third loading condition of group (a) of Fig. 5 and with reflective planes located on the front and back surfaces of the specimen; it is evident that the curves obtained with these two locations of the reflective plane are dramatically different. However, the experimental and computed curves coincide well with each other.

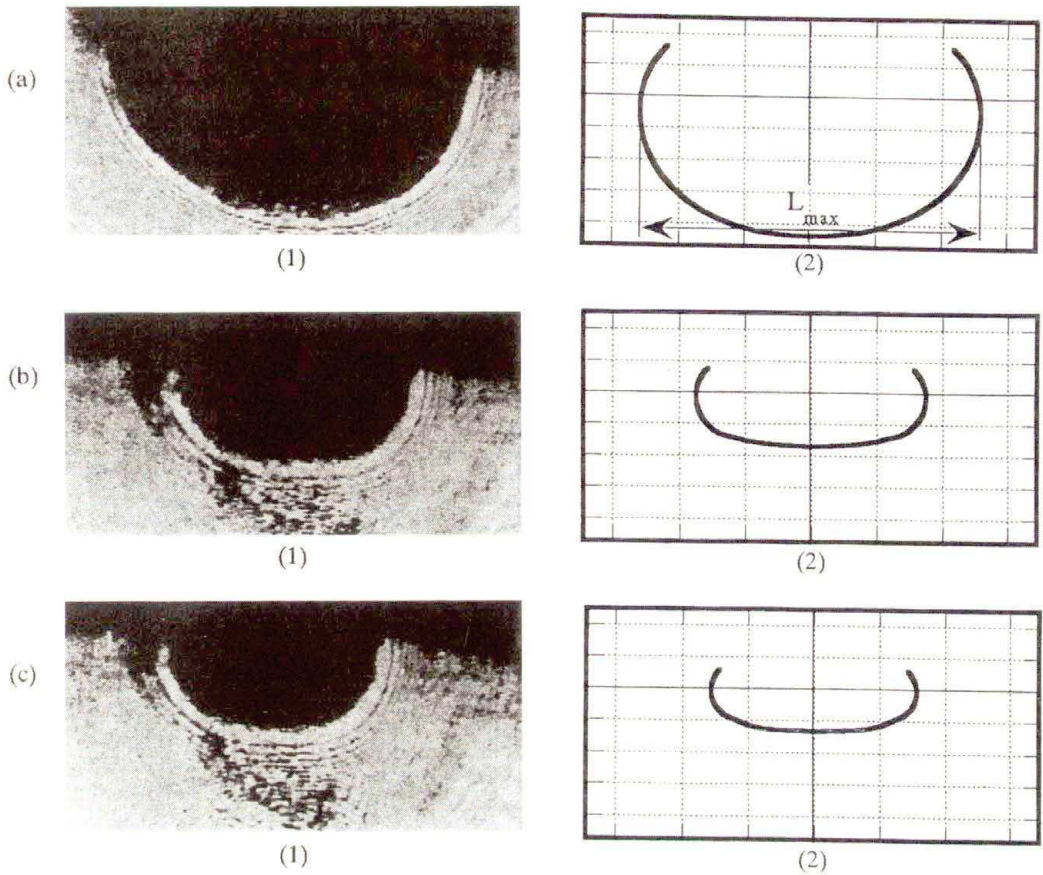


FIG. 8. Experimental and computed caustic curves for different locations ((a) the front layer, (b) the middle layer and (c) the rear layer) of the maximum load  $4\sigma$ .

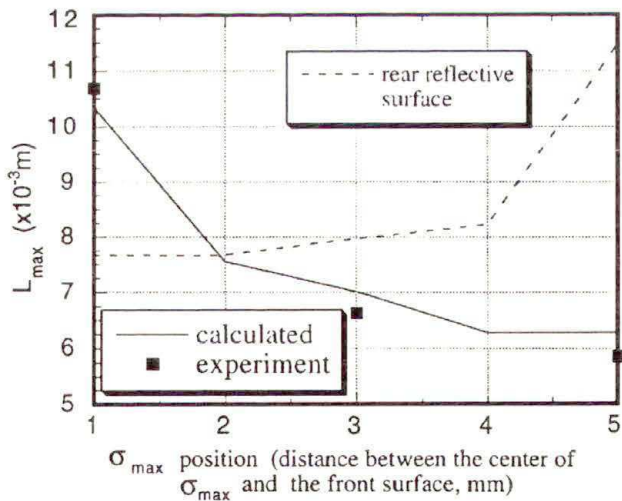


FIG. 9. Dependence of the size of the caustic curve upon the location of the maximum traction for two different positions of the reflective plane.

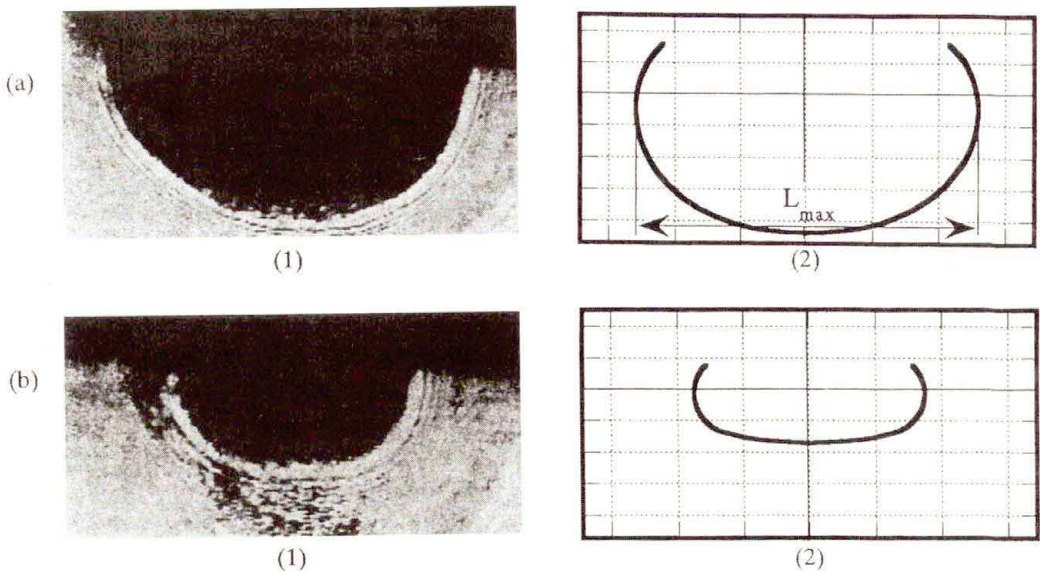


FIG. 10. Experimental and computed caustics for loading 3 (a) of Fig. 5 with (a) reflective plane located on the front surface of the plate, (b) reflective plane located on the rear surface of the plate.

## 5. A simple inverse problem

In applications one wishes to determine the externally applied load and/or the stress distribution from the knowledge of the shape and dimension of the caustics. However, if the external force pattern is known, its amplitude may be estimated from the dimensions of the caustic curve. We assume the load distribution  $a(1)$  of Fig. 5 with the reflective plane located on the front surface of the plate. In Table

Table 1. Comparison of the tractions computed from caustics and the applied tractions.

$P_1 : P_2 : P_3$	2:1:1	3:1:1	4:1:1
$D$ or $L_{\max}$ (mm)	7.82	9.22	10.69
Applied traction $\sigma$ MN/m <sup>2</sup>	2.00	2.00	2.00
Computed traction $\sigma_{\text{est}}$ MN/m <sup>2</sup>	2.15	2.15	2.26
Difference %	7.5	7.5	13.0

1 we have listed the measured  $L_{\max}$ , the traction computed from Eq. (2.23), and the traction applied in tests. The maximum difference between the computed and the applied tractions of 13% suggests that the method gives acceptable results.

Figure 11 shows contours of nondimensional principal stresses  $\sigma_1$  and  $\sigma_2$  obtained from the experimentally observed caustics. Here  $p_{est}$  ( $\text{MN}/\text{m}^2$ ) is the intensity of applied tractions estimated from Eq. (2.23) and the size of the caustic curve. These contours show high gradients of stress near the point where the applied traction jumps from zero to a finite value.

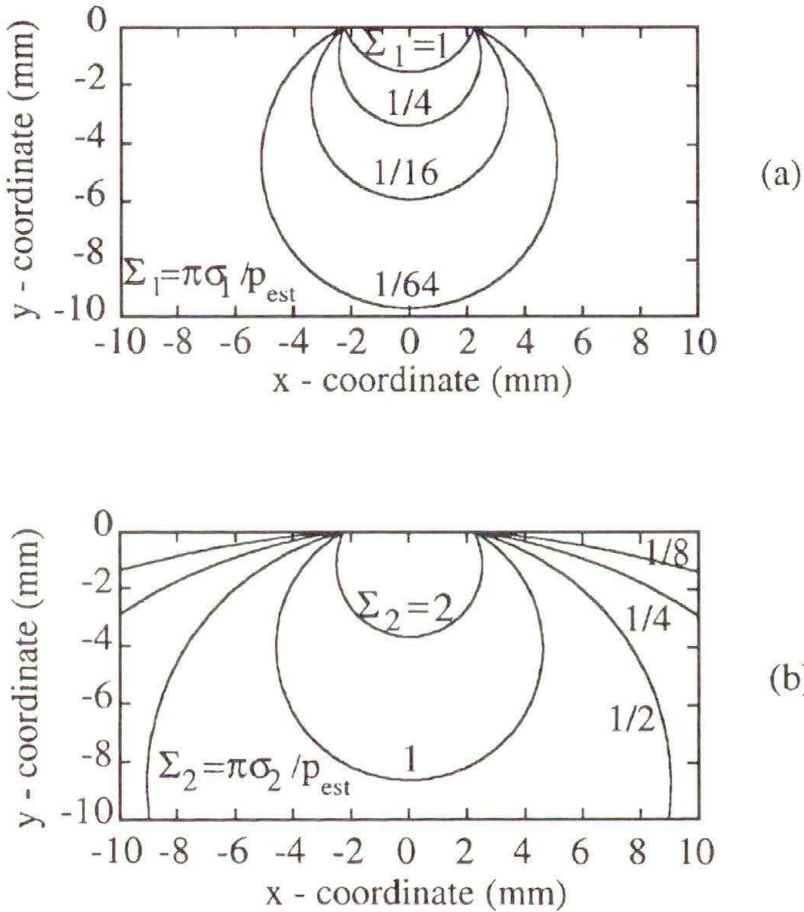


FIG. 11. Distribution of nondimensional principal stresses.

## 6. Conclusions

We have studied some basic characteristics of caustics produced in a homogeneous and both optically and mechanically isotropic thin rectangular plate subjected to in-plane loads on two opposite edges, with the other two edges kept traction-free. The applied load is such that points on the central plane of the plate do not undergo any lateral displacement. The effects of different distributions of

the edge loads and the location of the reflective plane upon the caustics produced has been discussed. Computed shapes of caustics and their sizes have been found to compare well with those observed experimentally. The pattern of the caustic curves produced is found to depend strongly upon the location of the reflective plane; the shapes of caustic curves are quite different when the reflective plane abuts on the front or rear surface of the plate. The magnitude of the applied load influences strongly the size of the caustic produced if the reflective plane is located near the point of application of the peak load. An inverse problem of determining the applied tractions from the size of the caustic curve has also been studied.

### Acknowledgment

This work was partially supported by the U.S. Office of Naval Research grant N00014-94-1-1211 with Dr. Y. D. S. RAJAPAKSE as the program manager.

### References

1. P. MANOGG, *Anwendung der Schattenoptik zur Untersuchung der Zerreissvorgangs von Platten*, Dissertation, Freiburg, Germany 1964.
2. P.S. THEOCARIS, *Stress-singularities at concentrated load*, *Exp. Mech.*, **13**, 511–528, 1973.
3. P.S. THEOCARIS, *Stress-singularities due to uniformly distributed loads along boundaries*, *Int. J. Solids Structures*, **9**, 655–669, 1973.
4. J.F. KALTHOFF, *Experimental fracture dynamics*, Crack dynamics in metallic materials, Springer-Verlag, New York, 69–253, 1987.
5. A.S. KOBAYASHI, *Handbook on experimental mechanics*, Second revised edition, SEM, New York 1993.
6. M. BORN and E. WOLF, *Principles of optics*, Pergamon Press, Oxford 1959.

DEPARTMENT OF ENGINEERING SCIENCE AND MECHANICS  
VIRGINIA POLYTECHNIC INSTITUTE AND STATE UNIVERSITY, BLACKSBURG, VA, USA

and

DEPARTMENT OF MECHANICAL ENGINEERING  
MIE UNIVERSITY, TSU, JAPAN.

Received February 27, 1996; new version July 18, 1996.